

Measurement of the $^{12}\text{C}(^3\text{He}, \pi^+)^{15}\text{N}$ reaction cross section near threshold

J. Homolka, W. Schott, W. Wagner, and W. Wilhelm
Physik Department, Technische Universität München, Munich, West Germany

R. D. Bent, M. Fatyga, and R. E. Pollock
Indiana University Cyclotron Facility, Bloomington, Indiana 47408

M. Saber and R. E. Segel
Northwestern University, Evanston, Illinois 60201

P. Kienle
Gesellschaft für Schwerionenforschung, Darmstadt, West Germany

(Received 18 April 1988)

The pionic fusion reaction $^{12}\text{C}(^3\text{He}, \pi^+)^{15}\text{N}$ has been measured at 170.2 and 236.3 MeV bombarding energy using recoil detection. At $T_{^3\text{He}} = 170.2$ MeV the angle-integrated cross section for the population of both the $^{15}\text{N}_{\text{g.s.}}$ and a broad group of unresolved ^{15}N excited states between $E_x = 6$ and 10 MeV is less than 0.03 nb. At $T_{^3\text{He}} = 236.3$ MeV the total cross section summed over both groups is (0.8 ± 0.2) nb.

I. INTRODUCTION

The pionic fusion process has been studied by several groups, both experimentally¹⁻⁸ and theoretically.⁹⁻¹³ Measurements of exclusive $(^3\text{He}, \pi^\pm)$ reactions for various target nuclei between ^3He and ^{12}C at bombarding energies in the range of 235 and 283 MeV have been done at Orsay.¹⁻⁴ The $^3\text{He}(^3\text{He}, \pi^+)^6\text{Li}$ reaction has been measured at Saclay in the range of 350 and 600 MeV.⁵ In both experiments high-resolution magnetic spectrometers for momentum analysis of the pions have been used. The time reversal reaction $^6\text{Li}(\pi^+, ^3\text{He})^3\text{He}$ has been measured by groups at LAMPF (Ref. 6) and TRIUMF,⁷ at bombarding energies between 39 and 90 MeV using solid-state detector spectrometers to identify the two ^3He particles.

A surprisingly large cross section of 20 nb/sr was observed for the $^3\text{He}(^3\text{He}, \pi^+)^6\text{Li}$ reaction at $T_{^3\text{He}} = 283$ MeV. Much smaller cross sections were found for heavier targets: ^6Li (50 pb/sr) and ^{10}B (40 pb/sr) at the same bombarding energy, and ^{12}C (100 pb/sr) at 235 MeV, where the numbers in the parentheses are the differential cross section at $\theta_\pi(\text{lab}) = 20^\circ$ for transitions to the ground states of the corresponding fusion products.

In a theoretical calculation for these processes Klingenberg, Dillig, and Huber^{9,10} used a microscopic Δ -excitation model where the initial relative motion of the two colliding nuclei is coupled to the final pion field in a cooperative way. Their theory has been applied only to the ^3He induced pionic fusion reaction with a ^3He target nucleus. Germond and Wilkin^{11,12} have also described this reaction by means of a cluster model.

Kajino, Toki, and Kubo¹³ use an interacting cluster model where the high-momentum parts of the clustering components in the final nucleus cooperate with the rela-

tive motion in the entrance channel to permit coherent pion production. The model has been applied to pionic fusion reactions with ^3He projectiles and target nuclei ranging from ^4He up to ^{40}Ca .

Up to now enough data are available only for the $^3\text{He}(^3\text{He}, \pi^+)^6\text{Li}_{\text{g.s.}}$ reaction which can give a limited insight into the dependence of the pionic fusion process cross section on the energy above threshold. We have therefore studied the $^{12}\text{C}(^3\text{He}, \pi^+)^{15}\text{N}$ reaction as a function of the bombarding energy. Recently, the angle-integrated cross section (σ) for the $^{12}\text{C}(^3\text{He}, \pi^+)^{15}\text{N}$ reaction has been measured at the Indiana University Cyclotron Facility (IUCF) at 181.4 MeV bombarding energy⁸ using recoil detection. In this paper the results of two more measurements, at 170.2 and 236.3 MeV, are presented. The dependence of σ on the energy above threshold is discussed and compared with the energy dependence for the $^3\text{He}(^3\text{He}, \pi^+)^6\text{Li}_{\text{g.s.}}$ reaction.

II. EXPERIMENT

The recoil detection method for studying fusion-type reactions has been described in previous papers.^{8,14} In fusion reactions where light emitted particles carry off only a small fraction of the incident momentum, the heavy recoil products are confined to a narrow forward cone. Therefore, nearly all of the recoil ions can be analyzed with high efficiency by a large solid-angle magnetic spectrograph. By using a magnetic spectrometer, which measures $p/Q = Am_N v/Q$ where Q is the atomic charge, A the atomic number, and m_N the nucleon mass, in combination with a time-of-flight measurement of velocity (v), the ratio A/Q can be determined. From an energy-loss measurement ($\Delta E/\Delta x$) one obtains the nuclear charge, Z . Since Q , Z , and A are all integers, with $Q \leq Z$,

and only certain Z, A combinations are possible, these three measurements (p/Q , v and $\Delta E/\Delta x$) are sufficient to fix Z , A , and Q , and, therefore, p .

A beam of $^3\text{He}^{++}$ ions was accelerated to laboratory kinetic energies of 170.2 and 236.3 MeV in the Indiana University Cyclotron, and transported and focused to a 2 mm diameter spot on a $210 \mu\text{g}/\text{cm}^2$ carbon foil target located in the target chamber of the quadrupole-quadrupole-split-dipole (QQSP) magnetic spectrograph. At these bombarding energies, the $^{15}\text{N}_{\text{g.s.}}$ recoil ions from the $^{12}\text{C}(^3\text{He}, \pi^+)^{15}\text{N}$ pionic fusion reaction are emitted within forward cones of 54.8 and 125.2 mr opening angles, with kinetic energies between 30.8 and 38.4 MeV and between 36.8 and 60.8 MeV, respectively. The $^{15}\text{N}_{\text{g.s.}}$ ions emerge from the target as N^{7+} with probabilities between 0.5 and 0.6 and between 0.6 and 0.8, respectively. The $^{15}\text{N}^{7+}$ recoils are analyzed using the QQSP spectrograph. The QQSP has a large-momentum acceptance of $0.82 \leq p/p_0 \leq 1.37$ where p_0 is a reference momentum. The maximum angular acceptance relative to the QQSP axis is $\theta_{0\text{max}} = \pm 100$ mrad and $\Phi_{0\text{max}} = \pm 100$ mrad in the horizontal and vertical plane, respectively. The maximum solid angle is 35 msr. In the present work an aperture restricted $\Phi_{0\text{max}}$ to ± 50 mrad. The angular magnifications in the horizontal and vertical planes are 3.27 and 0.34, respectively, and the momentum resolution is $\Delta p/p = 1/1000$.

By measuring position (x) and direction angle (α) of the recoil ions at the spectrograph focal plane, the momentum per unit charge p/Q and the emission angle θ of the ions at the target can be determined. For reactions leading to a two-body final state the recoil products will lie on a half-ellipse-shaped contour in the (p, θ) plane. The position (x) and direction (α) of the recoils at the focal plane were measured by two transmission-type position-sensitive parallel-plate avalanche counters (PPAC), each with an active area of $60 \times 5 \text{ cm}^2$. The first detector was located in the spectrograph focal plane, while the second was 12 cm behind the focal plane. The angle α is related to the emission angle, θ , in the reaction plane by

$$\theta = (\alpha - \alpha_0)/R_{22} + \beta = \theta_0 + \beta, \quad (1)$$

where α_0 is the angle for particles which start along the QQSP axis ($\alpha_0 = 0.805$ rad), β an offset angle between the beam and the QQSP axis ($\beta = 84.65$ mr), and $R_{22} = 3.27$ the angular magnification in the horizontal plane. In Fig. 1, the kinematic loci in the $(p/p_0, \theta)$ plane for ^{15}N fusion products from the $^{12}\text{C}(^3\text{He}, \pi^+)^{15}\text{N}$ reaction at $T_{^3\text{He}} = 236.3$ MeV leading to the ground state (solid lines) and to the $E_x = 10$ MeV excited state of ^{15}N (dotted-dashed lines) are drawn. The ellipses have been calculated using a computer simulation program. The width in p is due to the energy loss of the recoils in the target corresponding to an energy spread of 3.3 MeV at the maximum recoil energy of 60.8 MeV. In the forward direction, a ^{15}N recoil in the least bound state (10 MeV) has only about 1.3 MeV less energy than a recoil ion in the ground state. Since θ is determined only by the angle θ_0 measured in the horizontal plane, the finite axial aperture

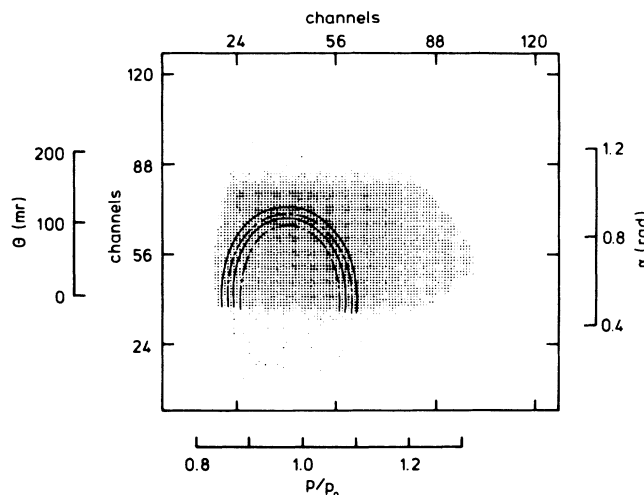


FIG. 1. Two-dimensional plot for reaction products in the $(\theta$ vs p/p_0) plane resulting from the bombardment of a ^{12}C target by 236.3 MeV ^3He particles. θ is the emission angle at the target, p is the momentum of the reaction product, and α is the angle of the particle relative to the spectrometer (QQSP) focal plane normal. The reference rigidity of the QQSP, expressed by the reference momentum p_0 of a particle with charge Q , is $p_0/Q = 0.571$ Tm. The edges of the data mark the boundaries of the acceptance of the QQSP detection system. The solid and dotted lines delineate the region where the $^{15}\text{N}_{\text{g.s.}}$ and the $^{15}\text{N}_{10.0}$ recoils from the $^{12}\text{C}(^3\text{He}, \pi^+)^{15}\text{N}$ reaction at $T_{^3\text{He}} = 236.3$ MeV are expected.

$\Phi_{0\text{max}}$ makes θ somewhat uncertain, causing the width of the kinematic locus in θ . Thus, the curves for the ground state and for the bound excited states strongly overlap, and it is not possible to resolve various bound states.

Only a tiny fraction (ca. 10^{-8}) of the reaction products which pass through the focal plane are from two-body final states, since there is always a high rate of spallation products which reach the detector in a broad momentum band. Therefore, good discrimination in the detection system is required. If θ vs p/p_0 is plotted for the spallation product events with no further conditions ($A/Q, Z$), then the sharp edges of the two-dimensional histogram mark the boundaries of the acceptance of the detecting system (cf. Fig. 1). The acceptance is limited by the QQSP beam optics and the detector geometry.

By dividing p/Q (determined from x) by the ion velocity (determined from the ion time-of-flight through the spectrometer), A/Q could be determined with a resolution of about 1%. The flight time exceeded the 67 ns burst spacing of the cyclotron beam, giving rise to a discrete ambiguity in the A/Q determination. The flight time between the two PPAC gave a second A/Q determination (with about 10% resolution) which removed this ambiguity and provided a second identification constraint. The atomic number Z of the recoil ion was determined by measuring the energy loss in a gas proportional counter (PC) with an active area of $60 \times 5 \text{ cm}^2$ mounted immediately behind the second PPAC.

Figure 2 shows the number of events as a function of

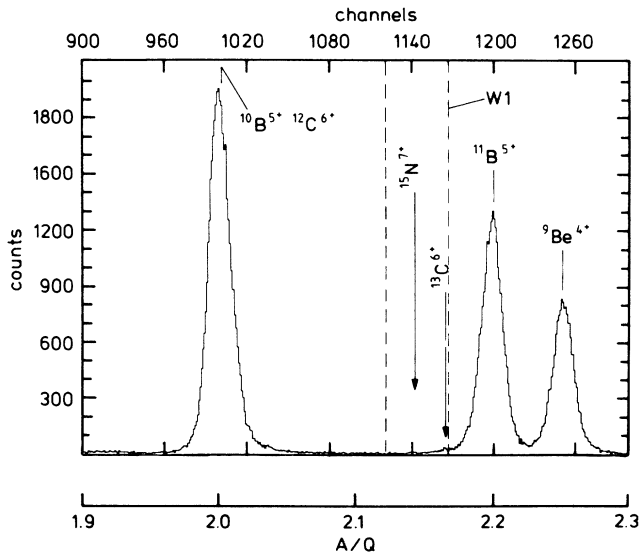


FIG. 2. Number of events vs A/Q . The rf pulse selecting condition has been applied. The window $W1$ (dotted line) was used to select the $^{15}\text{N}^{7+}$ ($A/Q=2.143$) events.

A/Q . The condition for selecting the correct time-of-flight stop pulse of the cyclotron rf has been applied. The spectrum contains intense lines of spallation products, ^9Be , ^{10}B , ^{11}B , and ^{12}C . The α particles, which produced a smaller signal in the PC, were eliminated by means of a threshold. The window $W1$ for the selection of $^{15}\text{N}^{7+}$ recoils is drawn in Fig. 2. They had to be separated from

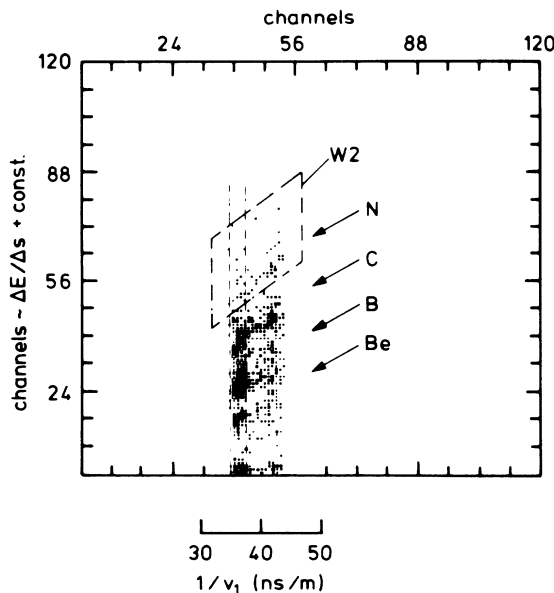


FIG. 3. Two-dimensional plot of the energy loss $\Delta E/\Delta s$ in the proportional counter, corrected for the path length through the counter, vs $1/v_1$, where v_1 is the velocity through the spectrometer. Only events which fulfill the rf pulse selecting condition and are within $W1$ (Fig. 2) are included. Groups of different Z are separated. The window $W2$ around ^{15}N recoil ions from the $^{12}\text{C}(^3\text{He},\pi^+)^{15}\text{N}$ reaction is shown.

much stronger groups of $^{13}\text{C}^{6+}$ and $^{11}\text{B}^{5+}$ ions. This is done using the window $W2$ in a plot where the specific energy loss, as deduced from the proportional counter signal, is plotted as a function of the inverse velocity of the ion between the target and the first PPAC. The window $W1$ and the rf pulse selection were used as conditions on the events shown in Fig. 3. The groups with different Z are well separated. One notes a weak group of particles with the largest energy loss, which is assigned to ^{15}N . The figure contains a substantial number of less heavily ionizing ^{13}C particles, which originate from the one-neutron transfer reaction on ^{12}C .

III. RESULTS

Figures 4(a) and (b) show scatter plots of ^{15}N recoils as a function of their emission angle, θ , and relative momentum, p/p_0 , for 236.3 and 170.2 MeV bombarding energy, respectively. The plots were made with sorting conditions requiring $A/Q=2.143$ and $Z=7$ to be satisfied, as indicated by the windows $W1$ and $W2$ shown in Figs. 2

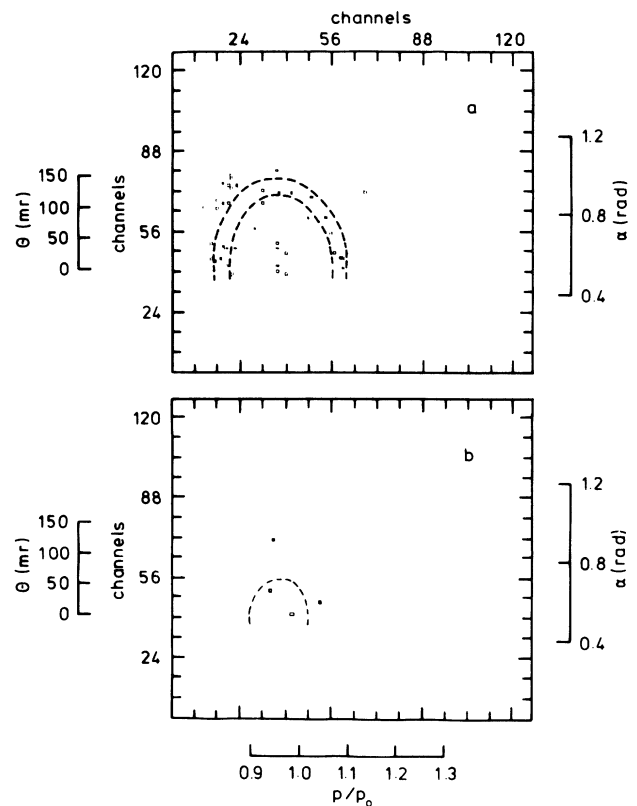


FIG. 4. Two-dimensional plots of ^{15}N recoil events in the θ vs p/p_0 plane which were obtained with the rf pulse selecting condition and the conditions $W1$ and $W2$. (a) Bombarding energy $T_{^3\text{He}}=236.3$ MeV, $p_0/Q=0.571$ Tm. The dashed lines delineate the region where ^{15}N recoils from the $^{12}\text{C}(^3\text{He},\pi^+)^{15}\text{N}$ reaction with excitation energies in the range $E_x=0, \dots, 10$ MeV are expected. (b) $T_{^3\text{He}}=170.2$ MeV, $p_0/Q=0.482$ Tm. The dashed line marks the outer boundary of the region for the ^{15}N recoils with $E_x=0, \dots, 10$ MeV. The inner boundary has shrunk to a dot in the center of the outer boundary ellipse.

and 3. These data were taken in 9–10 h runs with an average beam current of about 100 particle nanoamps. The elliptical curves are the predicted boundaries of the kinematic loci for the ^{15}N fusion products from the $^{12}\text{C}(^3\text{He}, \pi^+)^{15}\text{N}$ reaction in the excitation energy range $E_x = 0 \dots 10$ MeV. For $T_{3\text{He}} = 170.2$ MeV [Fig. 4(b)] the ellipses become small and the inner boundary of the locus shrinks to a point in the center of the outer ellipse. The spectrograph was set so that the beam entered at an angle $\beta = 84.65$ mr relative to the optical axis; consequently, the lower part of the kinematic loci is truncated by the entrance collimator. The Z identification does not completely separate the ^{13}C from the ^{15}N events of interest causing some background counts in the p/p_0 - θ plane. The resulting angle-integrated cross sections (σ) are given in Table I. The range of bound states is subdivided into two parts with $E_x = 0$ and $E_x \geq 6$ MeV, respectively.⁸ For $T_{3\text{He}} = 236.3$ MeV, the events are summed over the two E_x ranges due to lack of energy resolution. There are events in Fig. 4(a) distributed along the whole kinematic locus with perhaps some more on the low-momentum side suggesting a fairly isotropic angular distribution, with perhaps some peaking in the forward direction. For $T_{3\text{He}} = 170.2$ MeV, only two events are detected within the kinematically allowed region. From these, upper limits of the cross sections can be determined.

IV. DISCUSSION

In Fig. 5 all reported differential cross sections ($d\sigma/d\Omega$) are drawn as a function of the pion c.m. energy (T_π) for the $^3\text{He}(^3\text{He}, \pi^+)^6\text{Li}_{\text{g.s.}}$ (solid circles) and the $^{12}\text{C}(^3\text{He}, \pi^+)^{15}\text{N}$ reactions (open circles). The solid circles and solid rhombs denote $d\sigma/d\Omega$ measurements of the $^3\text{He}(^3\text{He}, \pi^+)^6\text{Li}_{\text{g.s.}}$ reaction from Orsay² and Saclay,⁵ the solid squares and solid triangles were obtained from $d\sigma/d\Omega$ data of the time reversal $^6\text{Li}(\pi^+, ^3\text{He})^3\text{He}$ reaction from LAMPF (Ref. 6) and TRIUMF,⁷ respectively. The data from Saclay are interpolated for the pion c.m. angle 30° . The open triangles denote $d\sigma/d\Omega$ values of the $^{12}\text{C}(^3\text{He}, \pi^+)^{15}\text{N}$ reaction, where $d\sigma/d\Omega$ was obtained from the measured, angle-integrated cross section σ (cf. Table I) by $d\sigma/d\Omega = \sigma/4\pi$, assuming isotropy. The results at $T_\pi \approx 5$ and 60 MeV are from this paper, the value at 15 MeV was measured previously at IUCF.⁸ The open circle denotes a $d\sigma/d\Omega$ measurement of the

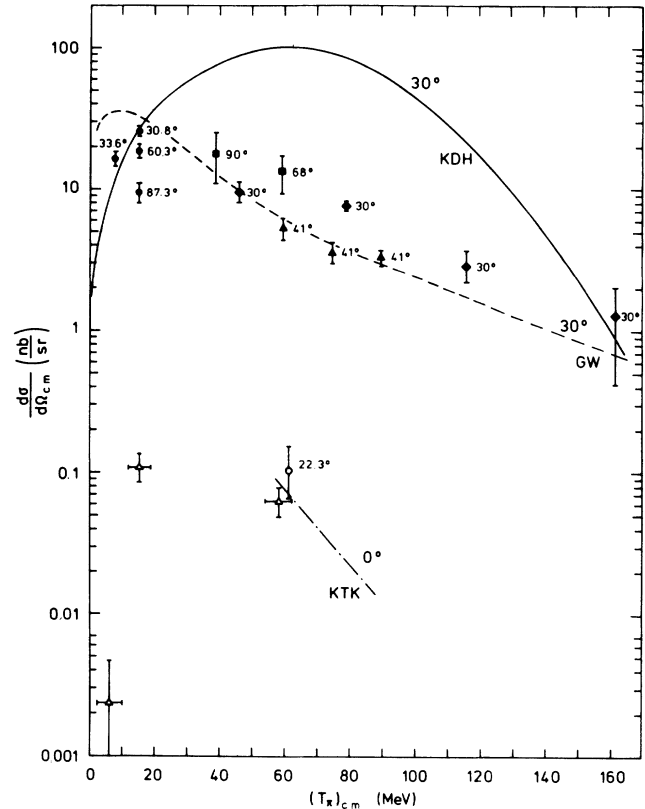


FIG. 5. Differential cross section ($d\sigma/d\Omega_{\text{c.m.}}$) of pionic fusion reactions vs center-of-mass pion energy (T_{π^+})_{c.m.}. The points denote measurements, the curves theoretical calculations. The pion emission angle (θ_{π^+})_{c.m.} of the $d\sigma/d\Omega_{\text{c.m.}}$ value is marked in degrees. Data points without angles denote $d\sigma/d\Omega_{\text{c.m.}}$ values which were obtained from the measured angle-integrated cross section σ by assuming isotropy. $^3\text{He}(^3\text{He}, \pi^+)^6\text{Li}_{\text{g.s.}}$: the solid circles, rhombs, squares, and triangles, are from Refs. 2, 5, 6, and 7, the solid and dashed curves were taken from Refs. 10 and 5, respectively. $^{12}\text{C}(^3\text{He}, \pi^+)^{15}\text{N}$: open triangles at (T_{π^+})_{c.m.} ≈ 5 and 60 MeV are data from this work; the open triangle at 15 MeV is from Ref. 8; the open circle is from Ref. 4; the dashed-dotted line is from Ref. 13.

$^{12}\text{C}(^3\text{He}, \pi^+)^{15}\text{N}_{\text{g.s.}}$ reaction from Orsay.⁴

As the recoil detection with the present setup has a limited energy resolution, the angle-integrated cross section is summed over the ground state and a wide range of

TABLE I. Angle-integrated cross section of the $^{12}\text{C}(^3\text{He}, \pi^+)^{15}\text{N}$ reaction for different bombarding energies $T_{3\text{He}}$ corresponding to pion c.m. energies T_π , where the ^{15}N recoil has the excitation energy E_x . For $T_{3\text{He}} = 236.3$ MeV, σ is summed over the two E_x ranges. The results for $T_{3\text{He}} = 181.4$ MeV are from Ref. 8.

$T_{3\text{He}}$ (MeV)	170.2		181.4		236.3	
	T_π (MeV)	σ (nb)	T_π (MeV)	σ (nb)	T_π (MeV)	σ (nb)
E_x (MeV)						
0.0	10.1	≤ 0.03	19.0	≤ 0.08	62.3	
6.0, . . . , 10.0	~ 2	< 0.03	~ 12	1.3 ± 0.3	~ 54	0.8 ± 0.2

bound excited states. The three cross sections obtained for the $^{12}\text{C}(^3\text{He},\pi^+)^{15}\text{N}$ reaction follow a curve which is similar in energy dependence to that reported for the $^3\text{He}(^3\text{He},\pi^+)^6\text{Li}_{\text{g.s.}}$ reaction. However, the cross section of the pionic fusion reaction with the ^{12}C target is more than 2 orders of magnitude smaller than that with the ^3He target. For both reactions, the cross section rises rapidly above threshold and peaks at a pion c.m. energy of several tens of MeV. From the given data, there is a hint for a maximum of $\sigma(T_\pi)$ for the $^{12}\text{C}(^3\text{He},\pi^+)^{15}\text{N}$ reaction between 20 and 60 MeV.

Included in Fig. 5 are theoretical curves of $d\sigma/d\Omega$ of the $^3\text{He}(^3\text{He},\pi^+)^6\text{Li}_{\text{g.s.}}$ reaction by Huber *et al.*¹⁰ (KDH) and Germond and Wilkin (GW) (curve taken from Ref. 5) and of the $^{12}\text{C}(^3\text{He},\pi^+)^{15}\text{N}_{\text{g.s.}}$ reaction by Kajino *et al.*¹³ (KTK). For the last case, $d\sigma/d\Omega$ has been calculated only at $T_\pi=61.0$ and 85.4 MeV. In order to approximate the energy dependence $d\sigma/d\Omega(T_\pi)$, both points were connected by a straight line.

V. CONCLUSIONS

The angle-integrated cross section (σ) for the $^{12}\text{C}(^3\text{He},\pi^+)^{15}\text{N}$ reaction has been measured at about 5 and 60 MeV above threshold by detection of the ^{15}N recoil ions. The cross section summed over the bound states of ^{15}N is <0.03 nb at $T_\pi \approx 5$ MeV and 0.8 ± 0.2 nb at $T_\pi \approx 60$ MeV. The resolution of the system was not sufficient to distinguish individual states. The results obtained in the present work extend up to a pion energy of 60 MeV, the range over which the $^{12}\text{C}(^3\text{He},\pi^+)$ cross section remains over 2 orders of magnitude smaller than

that of the $^3\text{He}(^3\text{He},\pi^+)$ reaction.

The achievable energy resolution in the present experiment was limited by the energy spread caused by the energy loss of the recoil products in the target. A storage ring is presently under construction at IUCF which will use ultra thin targets for which the energy loss, and therefore the target contribution to the energy resolution, will be negligible. Under those conditions, it will be possible to achieve an energy resolution of one part in a thousand with the recoil technique and still have luminosities approximately 100 times larger than those possible with fixed targets where the energy loss of the recoil particles limits the target thickness. At the Gesellschaft für Schwerionenforschung Darmstadt (GSI), a synchrotron for accelerating heavy ions to relativistic energies and a heavy fragment separator which can be used as a spectrometer, are being constructed. By means of this facility pionic fusion with inverse kinematics, i.e., the $^3\text{He}(^{12}\text{C},^{15}\text{N})\pi^+$ reaction, can be studied. The recoil energy is then more than 500 MeV. With a target thickness of the order of 1 mg/cm² and an energy resolution of 0.5×10^{-3} , single-excited states will be observable.

ACKNOWLEDGMENTS

We would like to thank the Indiana University Cyclotron Facility (IUCF) staff for providing us with a proton beam of excellent quality. The help of T. Huppertz with the data analysis is gratefully acknowledged. This work was supported by the Bundesministerium für Forschung und Technologie, and the U.S. National Science Foundation.

¹Y. Le Bornec *et al.*, Phys. Rev. Lett. **47**, 1870 (1981).

²Y. Le Bornec and N. Willis, in *Pion Production and Absorption in Nuclei—1981 (Indiana University Cyclotron Facility)*, Proceedings of the Workshop on Pion Production and Absorption in Nuclei, AIP Conf. Proc. No. 79, edited by R. D. Bent (AIP, New York, 1982), p. 155.

³N. Willis *et al.*, Phys. Lett. **136B**, 334 (1984).

⁴L. Bimbot *et al.*, Phys. Rev. C **30**, 739 (1984).

⁵Y. Le Bornec *et al.*, Phys. Lett. **133B**, 149 (1983).

⁶P. D. Barnes *et al.*, Nucl. Phys. **A402**, 397 (1983).

⁷G. J. Lolos *et al.*, Phys. Lett. **126B**, 20 (1983).

⁸W. Schott *et al.*, Phys. Rev. C **34**, 1406 (1986).

⁹K. Klingenberg, M. Dillig, and M. G. Huber, Phys. Rev. Lett. **47**, 1654 (1981).

¹⁰M. G. Huber and K. Klingenberg, in *Pion Production and Ab-*

sorption in Nuclei—1981 (Indiana University Cyclotron Facility), Proceedings of the Workshop on Pion Production and Absorption in Nuclei, AIP Conf. Proc. No. 79, edited by R. D. Bent (AIP, New York, 1982), p. 389.

¹¹J.-F. Germond and C. Wilkin, Phys. Lett. **106B**, 449 (1981).

¹²J.-F. Germond and C. Wilkin, in *Pion Production and Absorption in Nuclei—1981 (Indiana University Cyclotron Facility)*, Proceedings of the Workshop on Pion Production and Absorption in Nuclei, AIP Conf. Proc. No. 79, edited by R. D. Bent (AIP, New York, 1982), p. 411.

¹³T. Kajino, H. Toki, and K. Kubo, Phys. Rev. C **35**, 1370 (1987).

¹⁴J. Homolka *et al.*, Nucl. Instrum. Methods, Phys. Res. A **260**, 418 (1987).

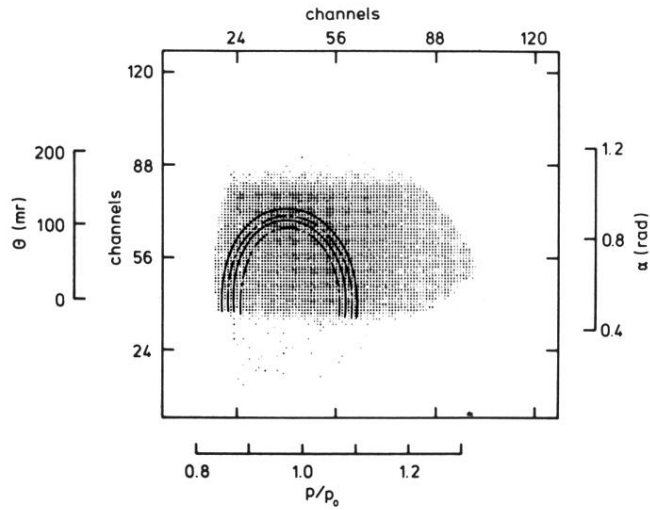


FIG. 1. Two-dimensional plot for reaction products in the (θ vs p/p_0) plane resulting from the bombardment of a ^{12}C target by 236.3 MeV ^3He particles. θ is the emission angle at the target, p is the momentum of the reaction product, and α is the angle of the particle relative to the spectrometer (QQSP) focal plane normal. The reference rigidity of the QQSP, expressed by the reference momentum p_0 of a particle with charge Q , is $p_0/Q=0.571$ Tm. The edges of the data mark the boundaries of the acceptance of the QQSP detection system. The solid and dotted lines delineate the region where the $^{15}\text{N}_{g.s.}$ and the $^{15}\text{N}_{10.0}$ recoils from the $^{12}\text{C}(^3\text{He},\pi^+)^{15}\text{N}$ reaction at $T_{^3\text{He}}=236.3$ MeV are expected.